TechnoChem
International Journal of TechnoChem Research
ISSN:2395-4248
www.technochemsai.com
Vol.02, No.03, pp 189-201, 2016

Rigid and Flexible docking studies on optically pure (*R,R*)- and (*S,S*)-1-Phenylpropane-1,2-diamines.

P. Yowan Jeba Raj, T. Vidhyasagar and K. Rajeswari*.

Department of Chemistry, Annamalai University, Annamalainagar - 608 002, India
***e-mail:rraajjii2006@gmail.com**

Graphical Abstract:

	Rigid Docking	*Flexible Docking*
2CSC	(*R,R*)-PPDA > (*S,S*)-PPDA	(*S,S*)-PPDA > (*R,R*)-PPDA
4CSC	(*S,S*)-PPDA > (*R,R*)-PPDA	(*R,R*)-PPDA > (*S,S*)-PPDA
3EWC	(*R,R*)-PPDA > (*S,S*)-PPDA	(*R,R*)-PPDA > (*S,S*)-PPDA
3EWD	(*R,R*)-PPDA > (*S,S*)-PPDA	(*R,R*)-PPDA > (*S,S*)-PPDA

	Rigid Docking	*Flexible Docking*
(R,R)-L	*3EWD > 3EWC > 2CSC > 4CSC*	*3EWC > 3EWD > 2CSC > 4CSC*
(S,S)-L	*4CSC > 3EWD > 3EWC > 2CSC*	*2CSC > 4CSC > 3EWC > 3EWD*

Abstract: The mixture of bio-active isomeric candidates, *viz.*, (*R,R*)- and (*S,S*)-1-Phenylpropane-1,2-diamines (1-PPDAs) were synthesized and their optical purity were achieved by optimized chiral transformation. The model chemistry for those (components) were docked with four different receptor models such as 2CSC, 4CSC, 3EWC and 3EWD. Two different docking modes, *viz.*, Rigid and Flexible were used for studying the docking interactions using Argus Lab 4.0. The interacting residues and their different representations were encountered using PyMOL viewer and the Ramachandran's plots for free protein model and that with specified interacting residues from the docked receptors (and their back-bone structure plots for residues) were visualized using Discovery studio software. The hydrophobicity plots for every successive 5-residue counts were also predicted for the selected receptor models to know their bio-molecular potency for best docking. The efficiencies towards the docking modes were well predicted. The overall reports concludes that, the efficiency of the flexible modes were higher than that of the rigid ones. The drug actions of the ligand candidates with the sarcoma receptors are higher than that of carcinoma receptors. Interestingly, most of the times, the binding poses for (*R,R*)-candidates were found to be higher than that of the other.

Key words: homo-dichiral diamines, chiral transformation, rigid docking, flexible docking, interacting residues.

1. Introduction:

The bio-activity of the structurally unsymmetrical (*R*,*R*)-dichiral vicinal diamines are biologically much more better/active than those having (*S*,*S*)-dichirallity. The platin type complexes having promising activity due to the configurations found in their constituted diamine functionalities were identified and their far better activities of the competitive candidates (homo-dichirals) were also investigated through a series of docking studies. The two different docking modes such as rigid and flexible were taken into account for studying the supramolecular interaction of the synthesized compounds towards the diseased cell receptor models. The designed models corresponds to the synthesized enantiomeric candidates were docked with the receptor models [1,2] such as 2CSC (sarcoma), 4CSC (sarcoma), 3EWC (carcinoma) and 3EWD (carcinoma). The receptor's binding domains with respect to the enantiomeric configurations were computed using Argus Lab 4.0 version [3].

2. Methodology:

2.1. Experimental:

Through optimized procedure [4-6], originating from the enantiomeric 4-piperidones, (2*R*,3*S*,6*S*) and (2*S*,3*R*,6*R*)-3-methyl-2,6-diphenylpiperidin-4-one, the final product – enantiomeric diamines: (1*R*,2*R*)- and (1*S*,2*S*)-1-Phenylpropane-1,2-diamine were synthesized through the enantiomeric 5-diazapanones, (2*S*,3*S*,6*S*) and (2*R*,3*R*,6*R*)-3-methyl-2,7-diphenyl-1,4-diazapan-5-one. The final enantiomeric diamines, *viz.*, (1*R*,2*R*)- and (1*S*,2*S*)-1-phenylpropane-1,2-diamines were resolved using chiral reagents [7]. The optically pure diamines, (1*R*,2*R*)- and (1*S*,2*S*)-1-phenylpropane-1,2-diamines were recrystallized using distilled water containing drops of hydrochloric acid.

2.2. Computational Methods:

All the receptors models (subjected for dockings) were downloaded from Protein Data Bank web page [8]. All the docking computations were carried out with Argus Lab 4.0.1 [3] version by using 'ArgusDock' as docking engine with Rigid [9] and Flexible [10,11] ligand's torsional docking modes. All the docking representations and their ligand's sites binding interactions were visualized using PyMOL viewer [12] whereas the 2D docking interaction plots, Ramachandran's plots [13] and the hydrophobicity plots were visualized using Discovery studio 2016 program package [14].

2.3. Protein clean-up & Ligand orientations:

All the receptors were tinkered using protein clean-up procedure. The previously bound ligand (Misc.) and the water (or solvent) molecules from the receptor's sites were removed by simple selection and deletion route. The ligand conformations were also considered as important for docking computations. For the flexible dockings, the torsional changes were allowed but not for the rigid dockings. The structure and the atom-label scheme for the ligands, ligand conformations during the course of the docking and the receptors surfaces (vacuum electrostatics and element-mapping surfaces) were displayed in **Fig. 1**, **2** and **3**, respectively.

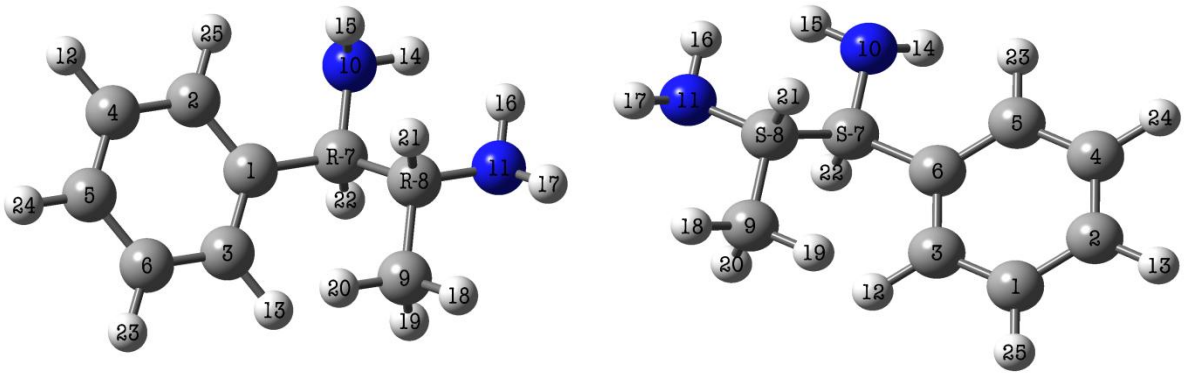

Fig. 1. Molecular structure and numbering scheme for (*R*,*R*)-1-PPDA (left) and (*S*,*S*)-1-PPDA (right).

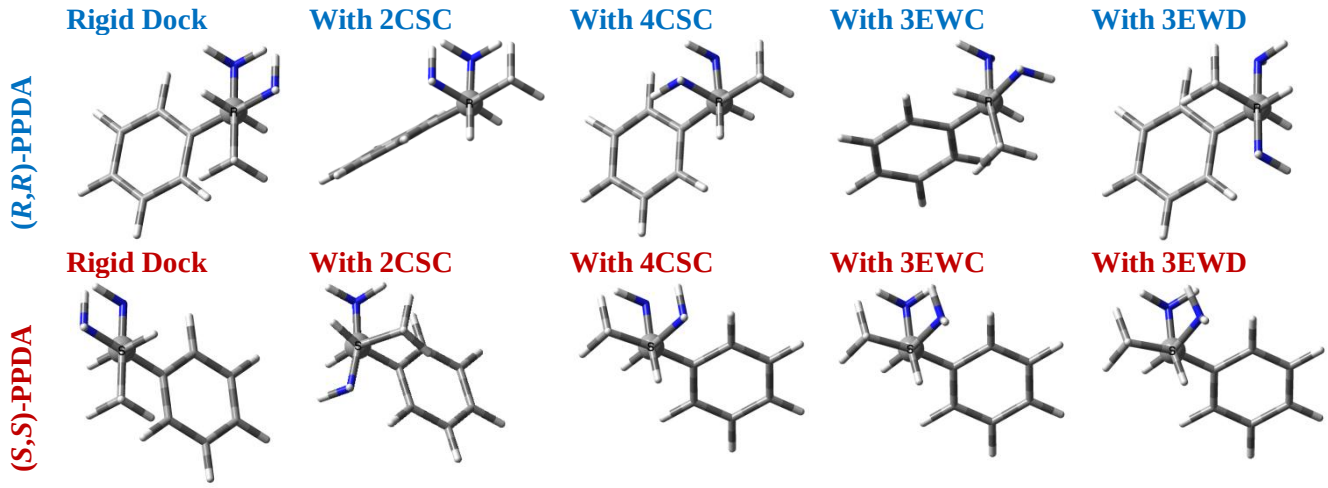

Fig. 2. Different ligand conformations adopted during Rigid (=input) and Flexible docking modes with different receptor models such as 2CSC, 4CSC, 3EWC and 3EWD.

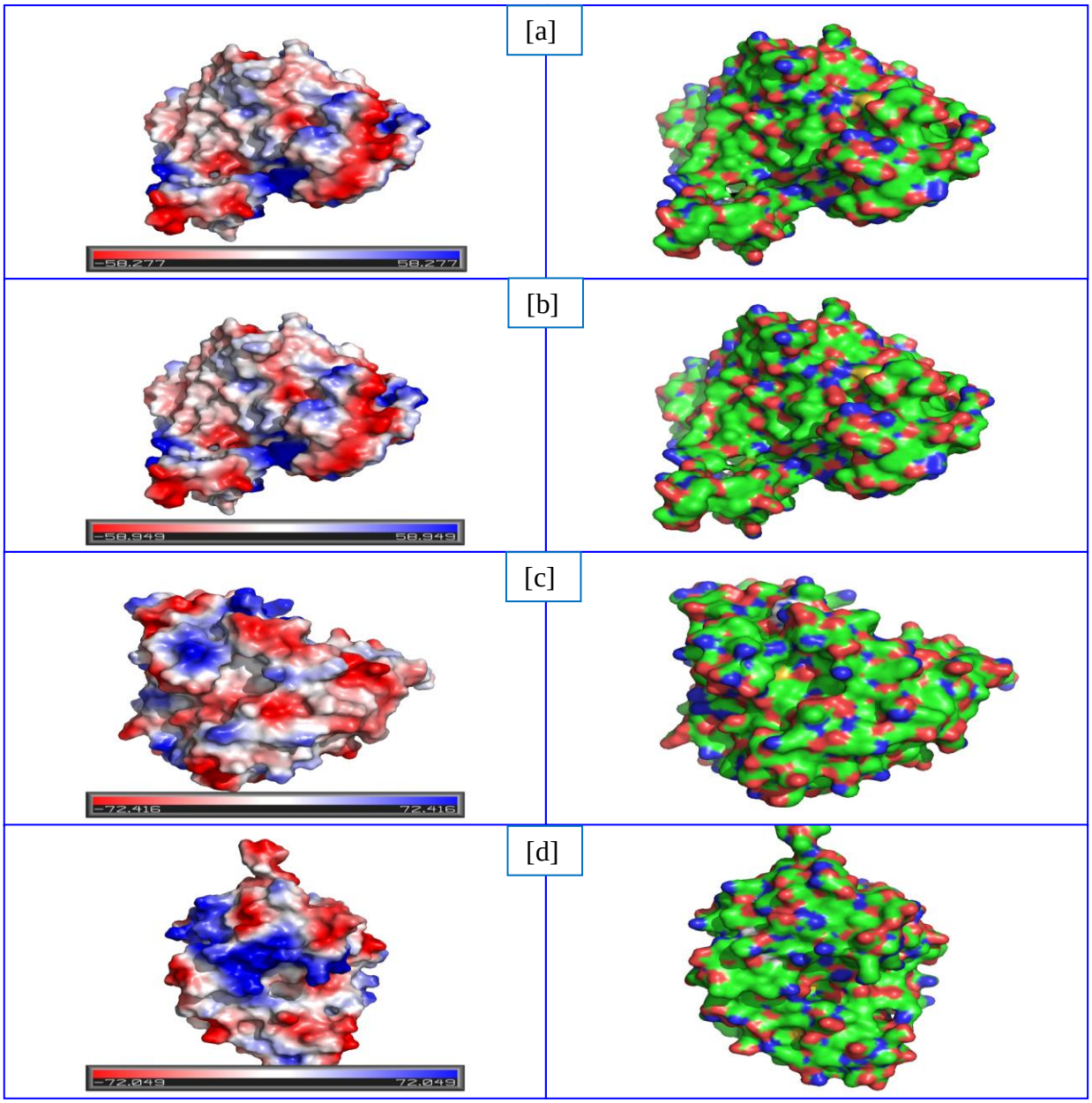

Fig. 3. Vacuum electrostatic surfaces (left) and Element-mapping surfaces (right) computed for (a) 2CSC, (b) 4CSC, (c) 3EWC and (d) 3EWD receptors.

Table 1. Ligand atom type informations during rigid and/or flexible dockings of (*R*,*R*)- and (*S*,*S*)-1-PPDA with selected receptors.

Atom label	Atom identifier of (*R*,*R*)-PPDA with,				Atom identifier of (*S*,*S*)-PPDA with,				Atom type
	2CSC	4CSC	3EWC	3EWD	2CSC	4CSC	3EWC	3EWD	
1C	3307	3307	2897	2955	3307	3307	2897	2955	Hydrophobic
2C	3308	3308	2898	2956	3308	3308	2898	2956	Hydrophobic
3C	3309	3309	2899	2957	3309	3309	2899	2957	Hydrophobic
4C	3310	3310	2900	2958	3310	3310	2900	2958	Hydrophobic
5C	3311	3311	2901	2959	3311	3311	2901	2959	Hydrophobic
6C	3312	3312	2902	2960	3312	3312	2902	2960	Hydrophobic
7C	3313	3313	2903	2961	3313	3313	2903	2961	Polar
8C	3314	3314	2904	2962	3314	3314	2904	2962	Polar
9C	3315	3315	2905	2963	3315	3315	2905	2963	Hydrophobic
10N	3316	3316	2906	2964	3316	3316	2906	2964	H-bond donor / acceptor
11N	3317	3317	2907	2965	3317	3317	2907	2965	H-bond donor / acceptor
12H	3318	3318	2908	2966	3318	3318	2908	2966	Atom type none
13H	3319	3319	2909	2967	3319	3319	2909	2967	Atom type none
14H	3320	3320	2910	2968	3320	3320	2910	2968	Atom type none
15H	3321	3321	2911	2969	3321	3321	2911	2969	Atom type none
16H	3322	3322	2912	2970	3322	3322	2912	2970	Atom type none
17H	3323	3323	2913	2971	3323	3323	2913	2971	Atom type none
18H	3324	3324	2914	2972	3324	3324	2914	2972	Atom type none
19H	3325	3325	2915	2973	3325	3325	2915	2973	Atom type none
20H	3326	3326	2916	2974	3326	3326	2916	2974	Atom type none
21H	3327	3327	2917	2975	3327	3327	2917	2975	Atom type none
22H	3328	3328	2918	2976	3328	3328	2918	2976	Atom type none
23H	3329	3329	2919	2977	3329	3329	2919	2977	Atom type none
24H	3330	3330	2910	2978	3330	3330	2910	2978	Atom type none
25H	3331	3331	2921	2979	3331	3331	2921	2979	Atom type none

Table 2. The values of different conformeric ligand torsions (in degrees) during rigid and flexible dockings with selected receptors.

Ligand (L)	Receptor	C6-C7-C8-C9	N10-C7-C8-C9	C6-C7-C8-N11	N10-C7-C8-N11
I	**Rigid dockings**				
(*R*,*R*)-PPDA	2CSC	59.829	179.897	179.966	-59.966
(*R*,*R*)-PPDA	4CSC	59.826	179.911	179.937	-59.978
(*R*,*R*)-PPDA	3EWC	59.848	179.963	179.916	-59.969
(*R*,*R*)-PPDA	3EWD	59.814	179.921	179.916	-59.977
(*S*,*S*)-PPDA	2CSC	-59.941	-179.988	179.970	59.922
(*S*,*S*)-PPDA	4CSC	-59.887	-179.992	-179.961	59.934
(*S*,*S*)-PPDA	3EWC	-59.904	179.997	179.993	59.894
(*S*,*S*)-PPDA	3EWD	-59.879	-179.996	-179.985	59.898
II	**Flexible dockings**				
(*R*,*R*)-PPDA	2CSC	-177.584	-57.514	-57.532	62.538
(*R*,*R*)-PPDA	4CSC	-58.836	61.262	61.232	-178.670
(*R*,*R*)-PPDA	3EWC	175.726	-64.168	-64.223	55.882
(*R*,*R*)-PPDA	3EWD	72.007	-167.861	-167.904	-47.773
(*S*,*S*)-PPDA	2CSC	46.385	-73.664	-73.753	166.198
(*S*,*S*)-PPDA	4CSC	-165.575	74.337	74.351	-45.736
(*S*,*S*)-PPDA	3EWC	-175.639	64.273	64.304	-55.783
(*S*,*S*)-PPDA	3EWD	-172.118	67.777	67.798	-52.308

3. Results and Discussion:

Optically pure diamine candidates were obtained through the designed procedure and followed by optimized chiral resolution methods. The model chemistry for the candidates were drawn and their biological performances towards carcinoma and sarcoma model receptors were performed theoretically using docking computations. Two docking modes were adopted for testing the browsing skill of the enantiomeric candidates to/over the receptor proteins. The performance activities of the isomeric candidates with carcinoma receptors are higher than that with sarcoma receptors. The occupancy or the induced fitting excellences during the flexible dockings are higher than that of the rigid dockings.

3.1. Ligand's Conformations:

Initially, when the ligands were subjected to dockings, by default, the atoms of the ligands were labeled by atomic identifier code and the atom types were assigned for the non-hydrogen atoms (**Table 1**) by ArgusDock engine. Different ligand conformations were adopted for flexible ligand dockings whereas none (except the input conformer) for the rigid dockings. The flexibility in torsional rotations exposed over the ligands made them attractive members for best biological actions (*ie.*, interactions) and are subjected to calculate their current structure-activity pharmacological scoring. The adopted ligand conformations during docking computations were presented in **Fig. 2**.

3.2. Rigid and Flexible dockings:

For rigid docking, no torsional changes were accounted for docking computations but those were considered for flexible dockings. The conformeric and configurational torsional angles of the ligands (**Fig. 2** & **Table 2**) and their atomic identifiers (**Table 1**) were analyzed for the flexible and the rigid dockings with different receptors. The flexible ligand docking patterns, ligand interacting sites (cartoon, dots and mesh view) with respect to 2CSC, 4CSC, 3EWC and 3EWD receptors were presented in **Fig. 4**. The 2D docking plots, that with secondary-assisted van der Waals interacting residues and the Ramachandran's plot's [13] for interacting residues for the flexible dockings were presented in **Fig. 5**. Rigid docking's 3D representations and their 2D interaction plots with Ramachandran's plots for the enantiomeric candidates with 2CSC, 4CSC, 3EWC and 3EWD were presented in **Fig. 6** and **Fig. 7**. It was observed that, the ligands bind with the receptor active sites for torsion-rigid ligand docking for the isomeric (enantiomeric) candidates are usually different; but that for the torsion-flexible ligand docking favors both enantiomers can even enter the same active domain, devoid of their configurational differences but due to conformational freedom, attracted the great interest for the idea of their self-extended drug actions. The interacting residues with the selected receptors, interaction types and interaction distances were presented in **Table 3**. The obtained consistency encourages the novelty of the present findings. The list of docking reports including the best docking pose energy were presented in **Table 4**.

3.3. Interacting residues and representations:

The (enantiomeric) model candidates with bio-receptor protein models after docking computations are having interactions with particular residues which actually found in receptor's active pockets. There are different interacting residues representations such as cartoons (pretty and publication views), dots and mesh surface views and were displayed in **Fig. 4** for every flexible docking pattern with receptors like 2CSC, 4CSC, 3EWC and 3EWD. The 2D plots for interacting residues and the van der Waals interacting residues too presented in **Fig. 5** for the flexible dockings with 2CSC, 4CSC, 3EWC and 3EWD receptors. The list of interacting residues with ligand's models for different receptor models during both rigid and flexible dockings were presented in **Table 3**. The picture-galleries of 3D docking patterns and 2D interaction plots for rigid docking studies for both the enantiomeric candidates with 2CSC, 4CSC, 3EWC and 3EWD receptors were collectively given in **Fig. 6** and **Fig. 7**.

3.4. Ramachandran's plots:

Ramachandran's plots [13] are the best illustrations for the interacting residues with the trail candidates from β-sheets, α-helix (right-handed), left-handed α-helix (L α-helix) and random-coil structural units of the protein backbones. The Ramachandran's plots for the total-residues, only-interacting residues of the docked protein receptors for flexible dockings and that for rigid dockings were presented in **Fig. 8**, **Fig. 5** and **Fig. 7**, respectively.

For flexible and rigid dockings, the Ramachandran plots with 2D interaction plots for the enantiomeric candidates with 2CSC, 4CSC, 3EWC and 3EWD receptors were collectively given in **Fig. 5** and **Fig. 7**, respectively.

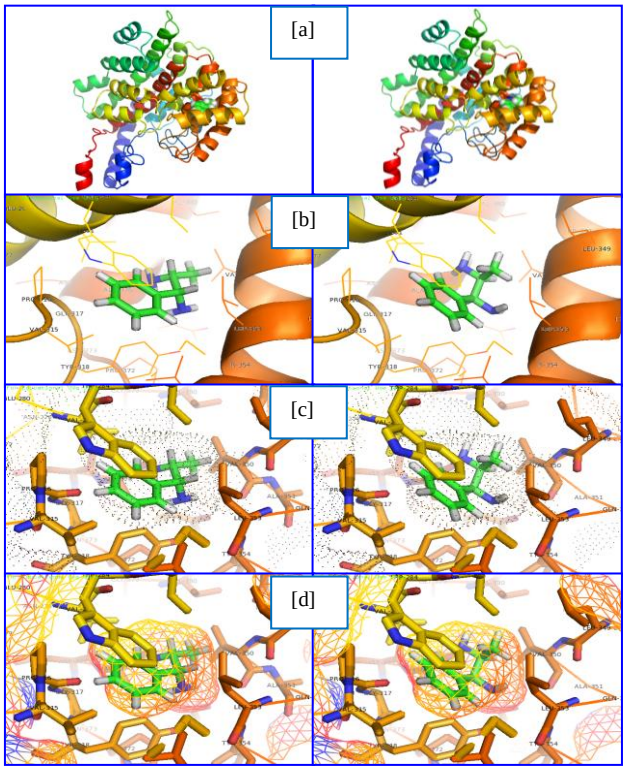

Flexible docking of (*R*,*R*)- and (*S*,*S*)-PPDA with 2CSC

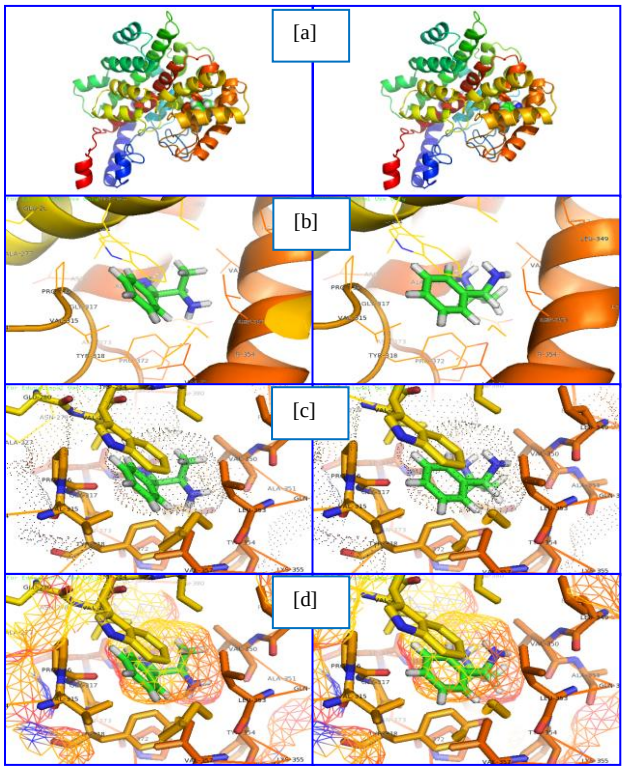

Flexible docking of (*R*,*R*)- and (*S*,*S*)-PPDA with 4CSC

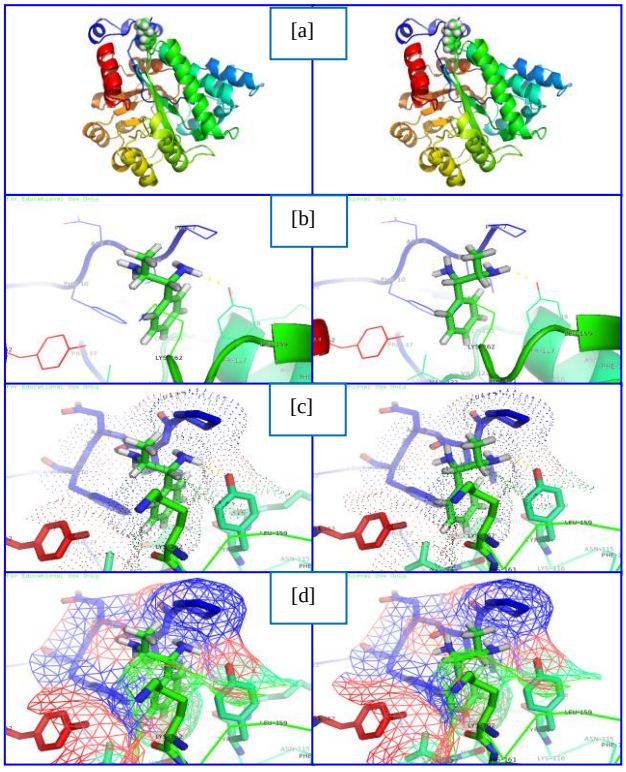

Flexible docking of (*R*,*R*)- and (*S*,*S*)-PPDA with 3EWC

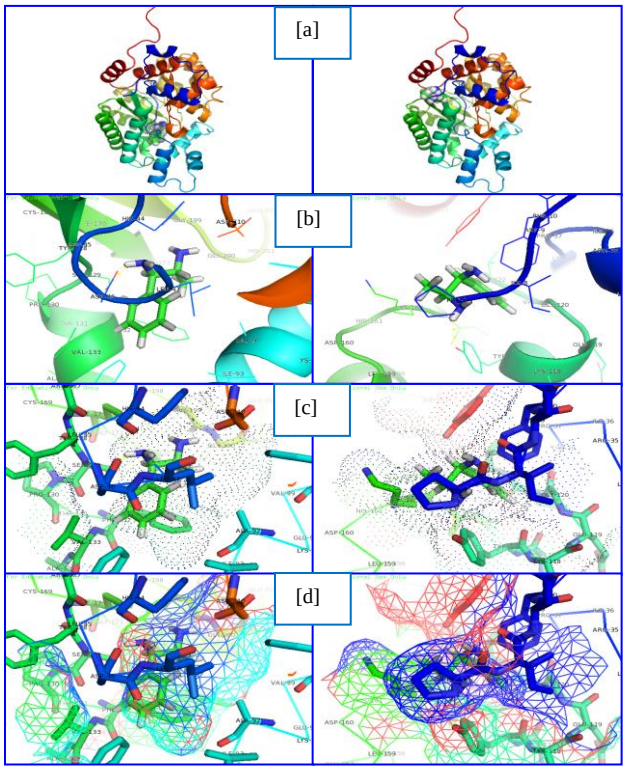

Flexible docking of (*R*,*R*)- and (*S*,*S*)-PPDA with 3EWD

Fig. 4. Flexible docking of (*R*,*R*)-1-PPDA (left) and (*S*,*S*)-1-PPDA (right) with 2CSC, 4CSC, 3EWC and 3EWD receptors: (a) 3D representations; Various interacting residue representations like (b) Cartoon views, (c) Dots views and (d) Mesh views.

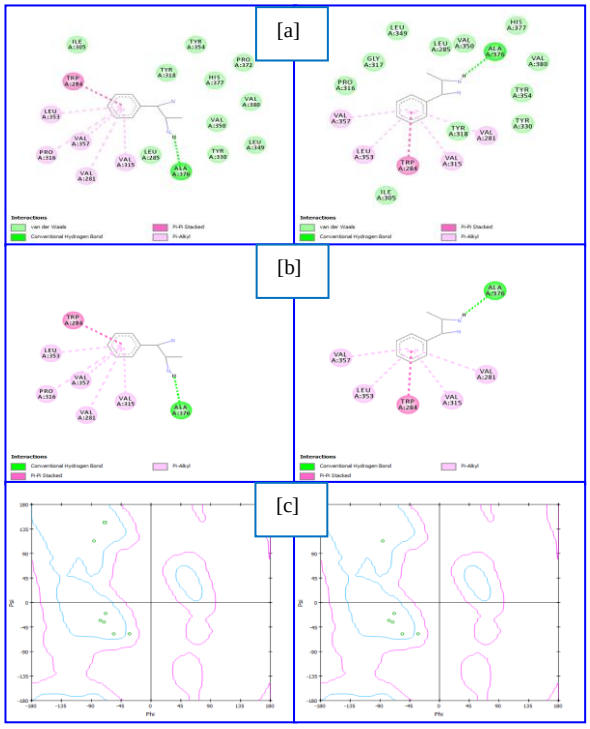

Flexible docking of (*R*,*R*)- and (*S*,*S*)-PPDA with 2CSC

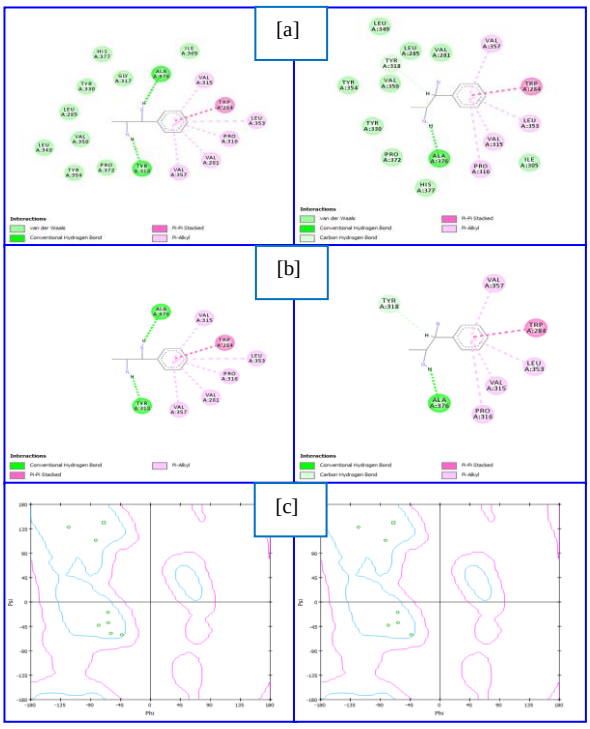

Flexible docking of (*R*,*R*)- and (*S*,*S*)-PPDA with 4CSC

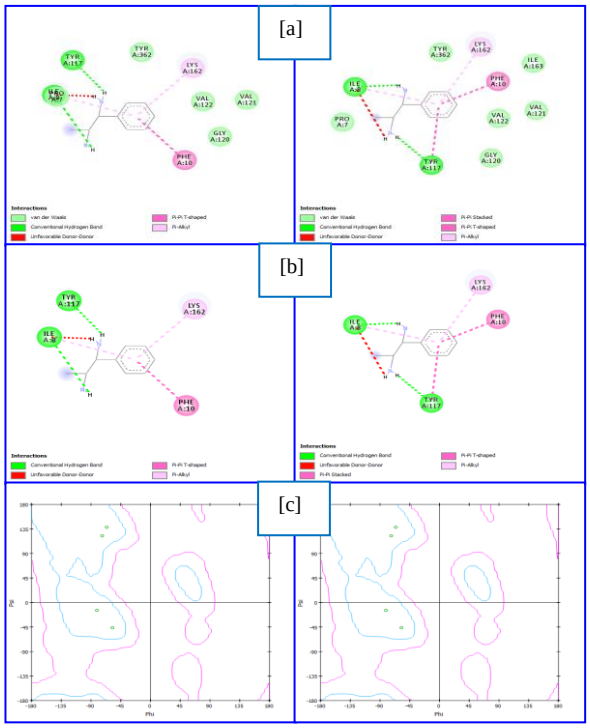

Flexible docking of (*R*,*R*)- and (*S*,*S*)-PPDA with 3EWC

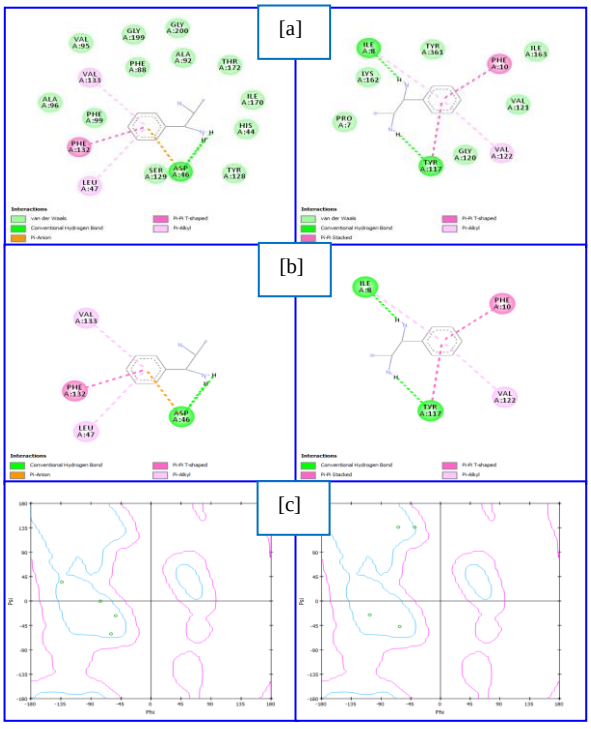

Flexible docking of (*R*,*R*)- and (*S*,*S*)-PPDA with 3EWD

Fig. 5. Flexible docking of (*R*,*R*)-1-PPDA (left) and (*S*,*S*)-1-PPDA (right) with 2CSC, 4CSC, 3EWC and 3EWD receptors: (a) 2D plots with van der Waals interacting residues, (b) 2D plots and (c) Ramachandran's plots.

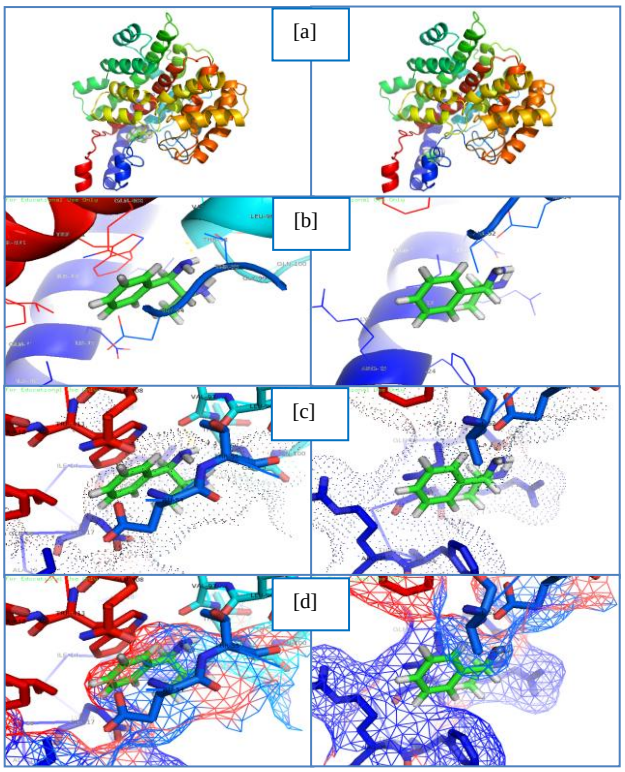

Rigid docking of (*R*,*R*)- and (*S*,*S*)-PPDA with 2CSC

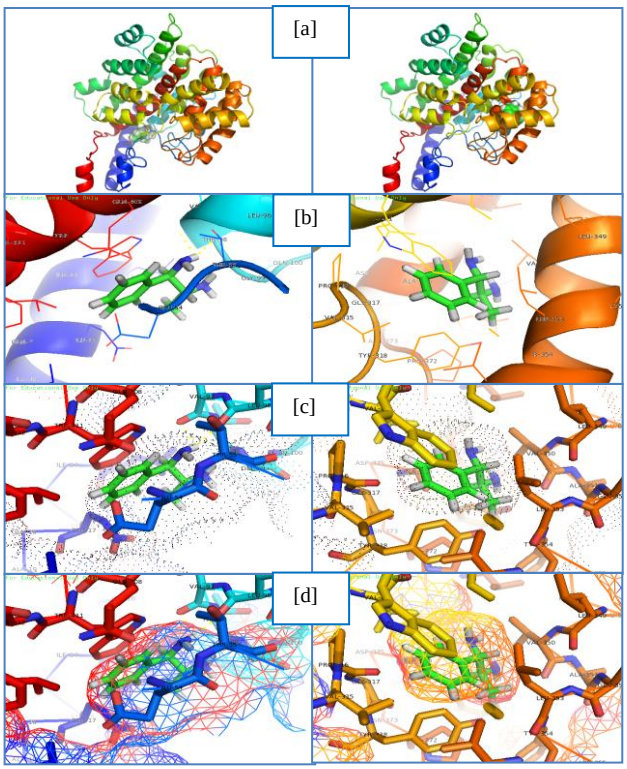

Rigid docking of (*R*,*R*)- and (*S*,*S*)-PPDA with 4CSC

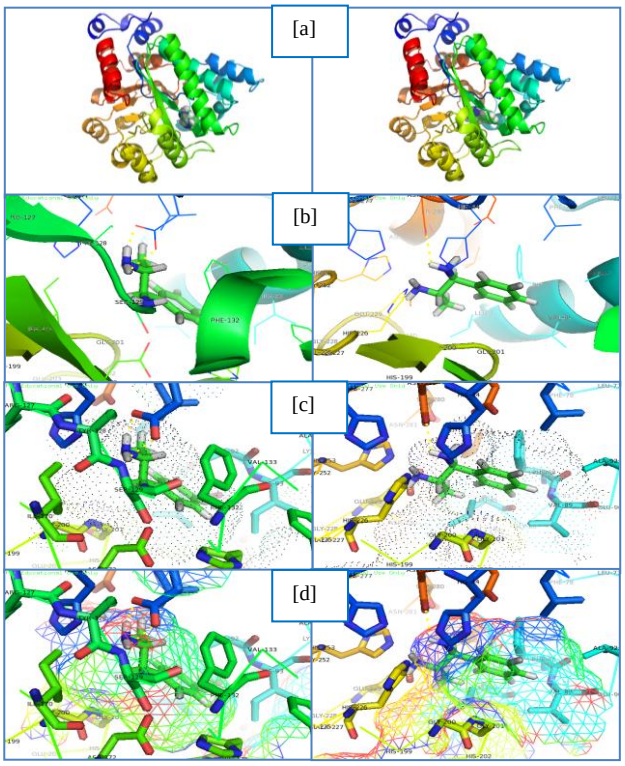

Rigid docking of (*R*,*R*)- and (*S*,*S*)-PPDA with 3EWC

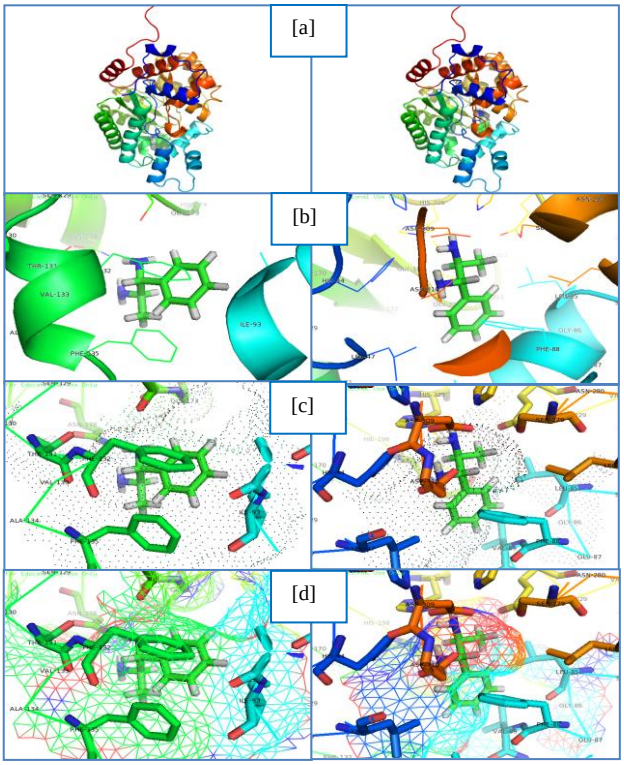

Rigid docking of (*R*,*R*)- and (*S*,*S*)-PPDA with 3EWD

Fig. 6. Rigid docking of (*R*,*R*)-1-PPDA (left) and (*S*,*S*)-1-PPDA (right) with 2CSC, 4CSC, 3EWC and 3EWD receptors: (a) 3D representations; Various interacting residue representations like (b) Cartoon views, (c) Dots views and (d) Mesh views.

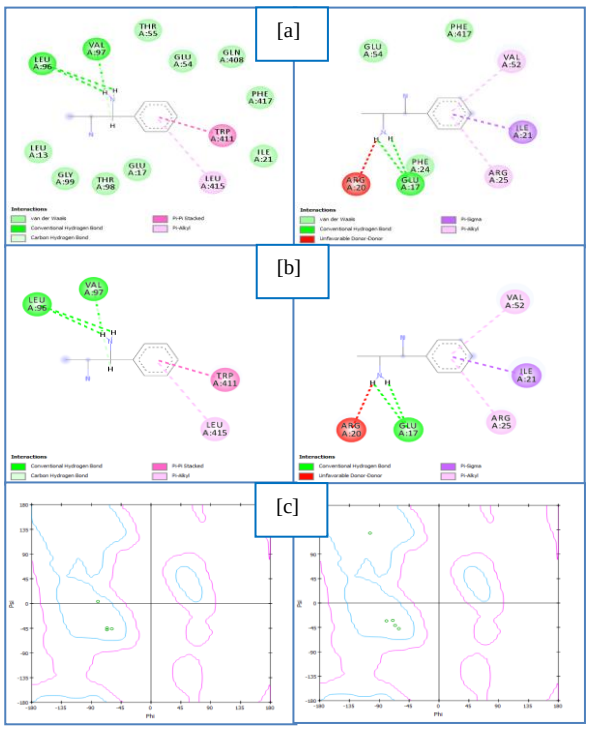

Rigid docking of (*R*,*R*)- and (*S*,*S*)-PPDA with 2CSC

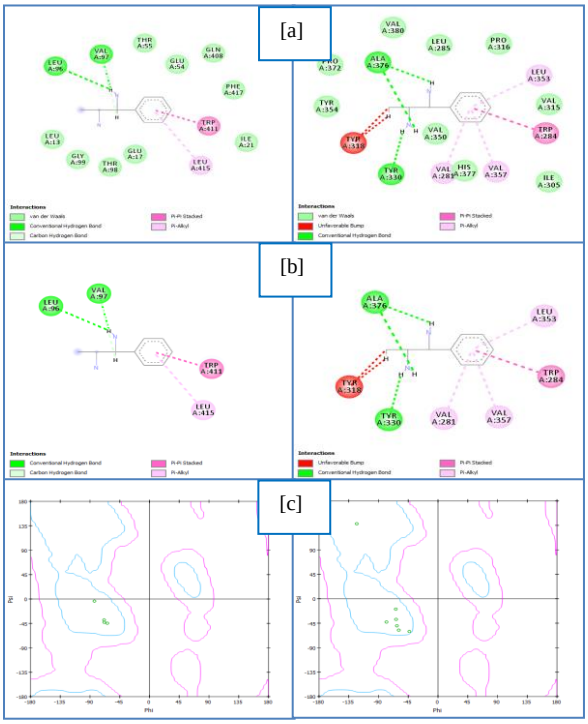

Rigid docking of (*R*,*R*)- and (*S*,*S*)-PPDA with 4CSC

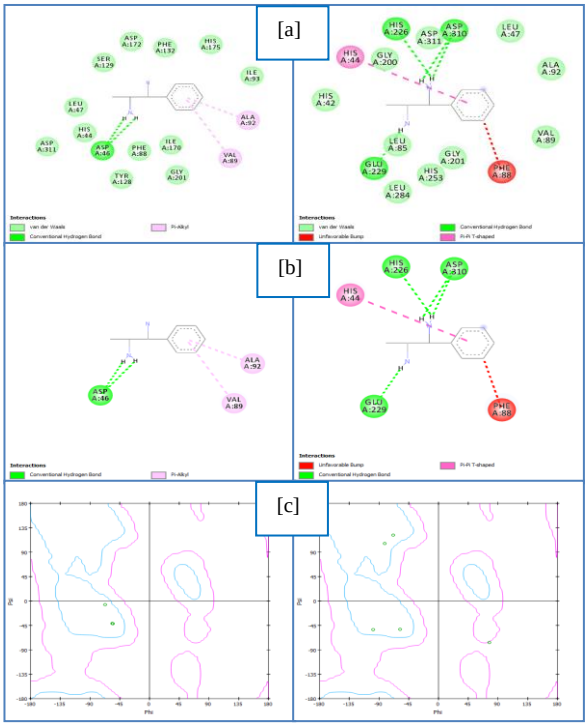

Rigid docking of (*R*,*R*)- and (*S*,*S*)-PPDA with 3EWC

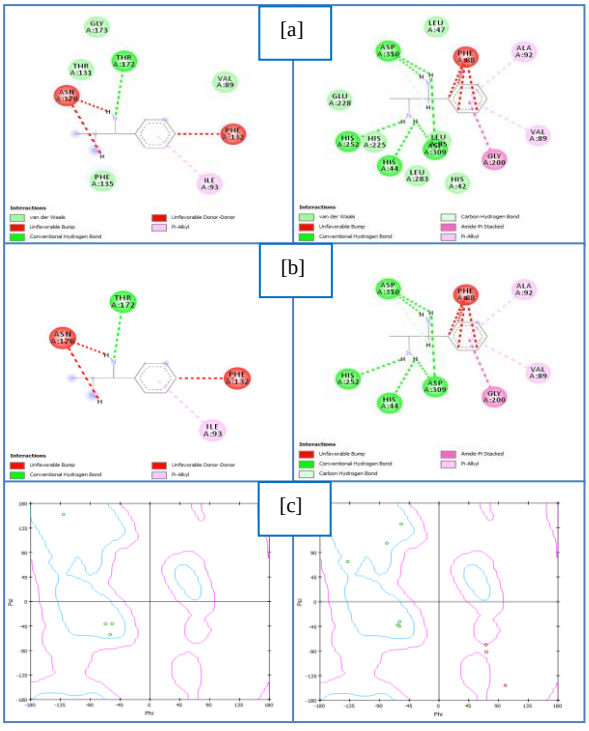

Rigid docking of (*R*,*R*)- and (*S*,*S*)-PPDA with 3EWD

Fig. 7. Rigid docking of (*R*,*R*)-1-PPDA (left) and (*S*,*S*)-1-PPDA (right) with 2CSC, 4CSC, 3EWC and 3EWD receptors: (a) 2D plots with van der Waals interacting residues, (b) 2D plots and (c) Ramachandran's plots.

3.5. Hydrophobicity Plots:

Both ligand's and receptor's hydrophobicities and their hydrophobicity interactions are considered to be the main key factors for Argus Lab dockings. The hydrophobicity plots are the typical plots for the illustration of the hydrophobic character of the receptor proteins with every successive 5-residue counts. The characteristic hydrophobicity plots and the receptor Ramachandran's plots for the protein receptors such as 2CSC, 4CSC, 3EWC and 3EWD were displayed in **Fig. 8**.

3.6. Relative Tolerances of the drug candidates:

The docking efficiency of the (*R*,*R*)-isomer is found better than that of (*S*,*S*)-isomer with all (the four) receptors except 4CSC during rigid docking mode and 2CSC on flexible mode. The obtained results were observed in accordance with the in-vitro anti-cancer activity [15] of the complex form of the title compounds. During flexible dockings, the drug action of the (*R*,*R*)-isomer is found higher for sarcoma receptors than that with the carcinoma receptors while the (*S*,*S*)-isomer follows the order just reverse to the previous. The orders for the enantiomeric Ligands Competitive Potency (LCP) and the subjected Receptors Competitive Potency (RCP) were pictorially represented in Graphical Abstract. The binding energy difference or biological interaction difference (BED/BID) between the two enantiomeric ligands (E-BID) and that between the two different docking modes (D-BID) were calculated and presented in **Table 5**. The E-BID and D-BID values provide the informations about the relative efficiency of enantiomeric and docking mode interactions relating to the drug actions of the candidates.

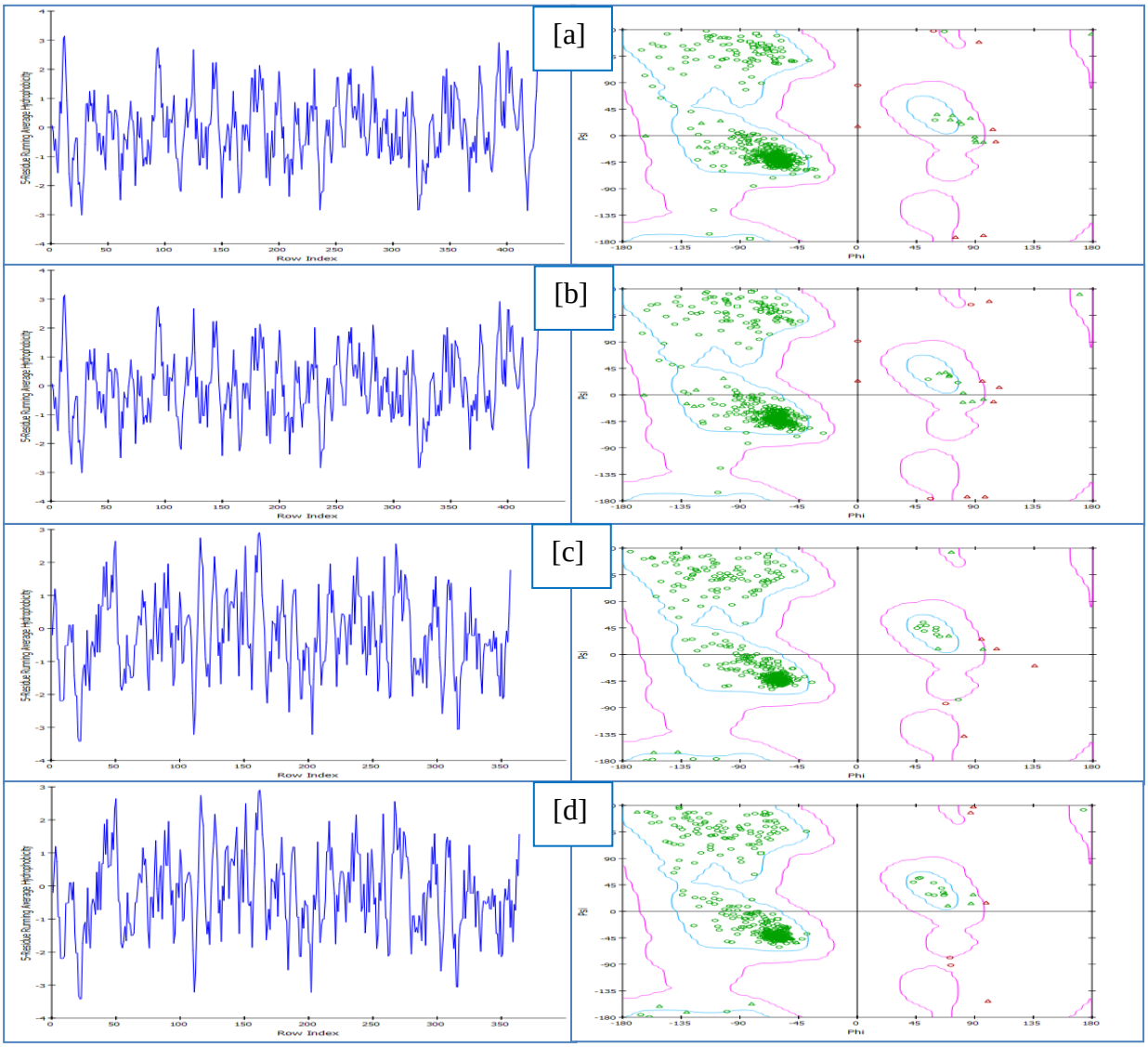

Fig. 8. The hydrophobicity (left) and Ramachandran's plot (right) computed for (a) 2CSC, (b) 4CSC, (c) 3EWC and (d) 3EWD receptors.

Table 3. List of interacting residues for Rigid and Flexible docking reports for (*R*,*R*)- and (*S*,*S*)-1-PPDA with carcinoma and sarcoma protein receptors.

Receptor	(*R*,*R*)-PPDA			(*S*,*S*)-PPDA		
	Residues	Interaction type	distance	Residues	Interaction type	distance
I	**Rigid dockings**					
2CSC	LEU 96	Hydrogen Bond	6.59	GLU 17	Hydrogen Bond	4.63
(6+9=15)	LEU 96	Hydrogen Bond	6.49	GLU 17	Hydrogen Bond	5.32
(6+3=9)	VAL 97	Hydrogen Bond	4.65	ARG 20	Donor-Donor (unfavorable)	2.84
	VAL 97	Hydrogen Bond	5.92	ILE 21	Pi-Sigma	3.94
	TRP 411	Pi-Pi Stacked	3.49	ARG 25	Pi-Alkyl	4.51
	LEU 415	Pi-Alkyl	7.11	VAL 52	Pi-Alkyl	6.71
4CSC	LEU 96	Hydrogen Bond	6.27	VAL 281	Pi-Alkyl	6.75
(5+9=14)	VAL 97	Hydrogen Bond	4.53	TRP 284	Pi-Pi Stacked	5.87
(9+9=18)	VAL 97	Hydrogen Bond	5.76	TYR 318	Donor-Donor (unfavorable)	5.23
	TRP 411	Pi-Pi Stacked	3.41	TYR 318	Donor-Donor (unfavorable)	5.34
	LEU 415	Pi-Alkyl	7.10	TYR 330	Hydrogen Bond	5.09
				LEU 353	Pi-Alkyl	4.36
				VAL 357	Pi-Alkyl	4.39
				ALA 376	Hydrogen Bond	4.22
				ALA 376	Hydrogen Bond	4.45
3EWC	ASP 46	Hydrogen Bond	3.83	HIS 44	Pi-Pi T-shaped	8.26
(4+12=16)	ASP 46	Hydrogen Bond	4.60	PHE 88	Bump (unfavorable)	3.71
(6+10=16)	VAL 89	Pi-Alkyl	6.26	HIS 226	Hydrogen Bond	5.40
	ALA 92	Pi-Alkyl	5.59	GLU 229	Hydrogen Bond	4.37
				ASP 310	Hydrogen Bond	4.59
				ASP 310	Hydrogen Bond	4.63
3EWD	ILE 93	Pi-Alkyl	6.40	HIS 44	Hydrogen Bond	5.06
(5+4=9)	PHE 132	Donor-Donor (unfavorable)	4.36	PHE 88	Bump (unfavorable)	3.73
(14+6=20)	THR 172	Hydrogen Bond	4.48	PHE 88	Bump (unfavorable)	4.18
	ASN 178	Donor-Donor (unfavorable)	4.29	PHE 88	Bump (unfavorable)	4.22
	ASN 178	Donor-Donor (unfavorable)	4.51	PHE 88	Bump (unfavorable)	4.42
				VAL 89	Pi-Alkyl	3.71
				ALA 92	Pi-Alkyl	6.27
				GLY 200	Amide-Pi Stacked	4.50
				HIS 252	Hydrogen Bond	5.09
				ASP 309	Hydrogen Bond	4.39
				ASP 309	Hydrogen Bond	4.22
				ASP 310	Hydrogen Bond	4.30
				ASP 310	Hydrogen Bond	4.51
				ASP 310	C---H Bond	5.45
II	**Flexible dockings**					
2CSC	VAL 281	Pi-Alkyl	5.74	VAL 281	Pi-Alkyl	4.54
(7+10=17)	TRP 284	Pi-Pi Stacked	5.57	TRP 284	Pi-Pi Stacked	4.13
(6+11=17)	VAL 315	Pi-Alkyl	6.49	VAL 315	Pi-Alkyl	5.19
	PRO 316	Pi-Alkyl	6.24	LEU 353	Pi-Alkyl	6.33
	LEU 353	Pi-Alkyl	4.33	VAL 357	Pi-Alkyl	6.78
	VAL 357	Pi-Alkyl	5.78	ALA 376	Hydrogen Bond	2.96
	ALA 376	Hydrogen Bond	3.22			
4CSC	VAL 281	Pi-Alkyl	5.11	TRP 284	Pi-Pi Stacked	5.48
(8+9=17)	TRP 284	Pi-Pi Stacked	5.83	VAL 315	Pi-Alkyl	4.25
(7+9=16)	VAL 315	Pi-Alkyl	5.95	PRO 316	Pi-Alkyl	5.47
	PRO 316	Pi-Alkyl	5.28	TYR 318	C---H Bond	5.49
	TYR 318	Hydrogen Bond	4.67	LEU 353	Pi-Alkyl	5.24
	LEU 353	Pi-Alkyl	5.37	VAL 357	Pi-Alkyl	4.26
	VAL 357	Pi-Alkyl	6.00	ALA 376	Hydrogen Bond	2.24
	ALA 376	Hydrogen Bond	2.33			
3EWC	PRO 7	Donor-Donor (unfavorable)	3.82	ILE 8	Hydrogen Bond	4.14
(6+4=10)	ILE 8	Hydrogen Bond	3.61	ILE 8	Pi-Alkyl	4.17
(7+6=13)	ILE 8	Pi-Alkyl	4.27	ILE 8	Donor-Donor (unfav)	3.56
	PHE 10	Pi-Pi T-shaped	6.41	PHE 10	Pi-Pi Stacked	5.50
	TYR 117	Hydrogen Bond	5.59	TYR 117	Hydrogen Bond	5.58
	LYS 162	Pi-Alkyl	4.83	TYR 117	Pi-Pi T-shaped	4.53
				LYS 162	Pi-Alkyl	6.08
3EWD	ASP 46	Hydrogen Bond	3.84	ILE 8	Hydrogen Bond	4.32
(6+12=18)	ASP 46	Hydrogen Bond	3.90	ILE 8	Pi-Alkyl	4.51
(6+6=12)	ASP 46	Pi-Anion	4.37	PHE 10	Pi-Pi Stacked	5.51
	LEU 47	Pi-Alkyl	5.29	TYR 117	Hydrogen Bond	5.36
	PHE 132	Pi-Pi T-shaped	4.36	TYR 117	Pi-Pi T-shaped	4.44
	VAL 133	Pi-Alkyl	6.09	VAL 122	Pi-Alkyl	5.51

Table 4. List of docking reports: numbers of ligand torsions, ligand extended root node radii, clustering and re-clustering poses, best ligand pose energy and docking run elapsed time.

Ligand (L)	Protein (or) Receptor (R)	No. of torsions		Ligand extended root node radii			Max. no. of poses	Clustering & re-clustering the final poses	Best ligand pose: energy (kcal/mol)	Docking run: elapsed time (sec)
		L	R	Primary (1°)	Secondary (2°)	Tertiary (3°)				
I	**Rigid dockings**									
(*R*,*R*)-PPDA	2CSC	0	0	4.19826	2.47291	1.58454	150	108 & 106	-9.10096	142
(*R*,*R*)-PPDA	4CSC	0	0	4.19826	2.47291	1.58454	150	109	-9.09133	85
(*R*,*R*)-PPDA	3EWC	0	0	4.19826	2.47291	1.58454	150	111	-9.2582	70
(*R*,*R*)-PPDA	3EWD	0	0	4.19826	2.47291	1.58454	150	117	-9.2891	59
(*S*,*S*)-PPDA	2CSC	0	0	4.20344	2.49554	1.56316	150	111	-9.02588	136
(*S*,*S*)-PPDA	4CSC	0	0	4.20344	2.49554	1.56316	150	112	-10.3505	138
(*S*,*S*)-PPDA	3EWC	0	0	4.20344	2.49554	1.56316	150	114	-9.08577	94
(*S*,*S*)-PPDA	3EWD	0	0	4.20344	2.49554	1.56316	150	113	-9.21728	89
II	**Flexible dockings**									
(*R*,*R*)-PPDA	2CSC	4	0	2.87397	2.17244	0.0134653	150	62	-9.90448	181
(*R*,*R*)-PPDA	4CSC	4	0	2.87397	2.17244	0.0134653	150	64	-9.90332	285
(*R*,*R*)-PPDA	3EWC	4	0	2.87397	2.17244	0.0134653	150	66 & 65	-9.77924	175
(*R*,*R*)-PPDA	3EWD	4	0	2.87397	2.17244	0.0134653	150	57	-9.62768	185
(*S*,*S*)-PPDA	2CSC	4	0	2.87394	2.17229	0.0134642	150	61	-9.9632	284
(*S*,*S*)-PPDA	4CSC	4	0	2.87394	2.17229	0.0134642	150	62	-9.79703	287
(*S*,*S*)-PPDA	3EWC	4	0	2.87394	2.17229	0.0134642	150	70	-9.67284	124
(*S*,*S*)-PPDA	3EWD	4	0	2.87394	2.17229	0.0134642	150	55	-9.44052	118

Table 5. The calculated values of enantiomeric-biological interaction difference (E-BIDs) and docking mode-biological interaction differences (D-BIDs) from the investigated docking scores.

Trial Ligand (L)	Receptor	Rigid	Flexible	D-BID[a]	Docking Mode	Receptor	(*R*,*R*)-PPDA	(*S*,*S*)-PPDA	E-BID[b]
(*R*,*R*)-PPDA	2CSC	-9.101	-9.9045	-0.8035	**Rigid**	2CSC	-9.101	-9.0259	-0.0751
(*R*,*R*)-PPDA	4CSC	-9.0913	-9.9033	-0.812	**Rigid**	4CSC	-9.0913	-10.351	1.2592
(*R*,*R*)-PPDA	3EWC	-9.2582	-9.7792	-0.521	**Rigid**	3EWC	-9.2582	-9.0858	-0.1724
(*R*,*R*)-PPDA	3EWD	-9.2891	-9.6277	-0.3386	**Rigid**	3EWD	-9.2891	-9.2173	-0.0718
(*S*,*S*)-PPDA	2CSC	-9.0259	-9.9632	-0.9373	**Flexible**	2CSC	-9.9045	-9.9632	0.0587
(*S*,*S*)-PPDA	4CSC	-10.351	-9.797	0.5535	**Flexible**	4CSC	-9.9033	-9.797	-0.1063
(*S*,*S*)-PPDA	3EWC	-9.0858	-9.6728	-0.5871	**Flexible**	3EWC	-9.7792	-9.6728	-0.1064
(*S*,*S*)-PPDA	3EWD	-9.2173	-9.4405	-0.2232	**Flexible**	3EWD	-9.6277	-9.4405	-0.1872

[a]D-BID → [Flexible docking]-[Rigid docking]; [b]E-BID → [(*R*,*R*)-PPDA]-[(*S*,*S*)-PPDA]

4. Conclusion:

The relative biological activities of the synthesized candidates by model chemistry were tested by docking computations with carcinoma and sarcoma protein receptor models using Argus Lab 4.0 docking. Two kinds of docking modes were employed for the docking computations. The torsional-rigid ligand conformations browse the receptor with maximum extent to achieve the best binding pose with perfect fitting. The flexible dockings showed better binding pattern when compared to that shown by rigid dockings. Configurational distinctions and conformational adaptations of ligands with receptors impart significant for their self-extended drug action. The Ramachandran's plot revealed that the interacting residues come from the original structural back-bone of the receptors. The candidates were found to be the best suited towards sarcoma receptors than carcinoma receptors. Furthermore, the (*R*,*R*)-isomer was found as the potential candidate than the (*S*,*S*)-isomer for the selected receptors.

Abbreviations:

PPDA, 1-Phenylpropane-1,2-diamine; *R*, *Rectus* ; *S*, *Sinister*; 3D, Three Dimensional; 2D, Two Dimensional; LCP, Ligands Competitive Potency; RCP, Receptors Competitive Potency; BED/BID, binding energy difference/biological interaction difference; D-BID, docking mode-biological interaction difference; E-BID, enantiomeric-biological interaction difference.

Acknowledgment

Financial support from UGC – New Delhi is gratefully acknowledged. Authors Dr. K. Rajeswari and Dr. T. Vidhyasagar are thankful to University Grants Commission, for providing fund and Mr. P. Yowan Jeba Raj is thankful to UGC for providing Project fellowship.

References:

1. Karpusas, M., Holland, D. and Remington, S.J. 1.9-Å Structures of Ternary Complexes of Citrate Synthase with D- and L-Malate: Mechanistic Implications. Biochemistry, 1991, 30: 6024–6031.
2. Ho, M.-C., Cassera, M.B., Madrid, D.C., Ting, L.-M., Tyler, P.C., Kim, K., Almo, S.C. and Schramm, V.L. Structural and Metabolic Specificity of Methylthiocoformycin for Malarial Adenosine Deaminases. Biochemistry, 2009, 48(40): 9618–9626.
3. Argus Lab 4.0.1., Mark Thompson and Planaria Software LLC, 2004.
4. Noller, C.R. and Baliah, V. The Preparation of Some Piperidine Derivatives by the Mannich Reaction. J. Am. Chem. Soc., 1948, 70(11): 3853–3855.
5. Kumar, S.S., Kavitha, H.P., Vennila, J.P., Chakkaravarthi, G. and Manivannan, V. 6-Methyl-2,7-diphenyl-1,4-diazepan-5- one. Acta Cryst., 2009, E65: o3211.
6. Thennarasu, S. and Perumal, P.T. An Efficient Preparation of 1,2-Diamino-1-phenylheptane. Molecules, 2002, 7: 487–493.
7. Froentjes, W. and Dijkema, K.M. On the resolution and properties of the mesoidic form of l-phenyl-l,2-diaminopropne. Recueil, 1943, 62(11): 723–728.
8. RCSB Protein Data Bank – RCSB PDB main page: http://www. rcsb.org/.
9. Oda, A.,Yamaotsu, N., Hirono, S., Watanabe, Y., Fukuyoshi, S. and Takahashi, O. Effects of initial settings on computational protein – ligand docking accuracies for several docking programs, Molecular Simulation, 2014, 1–8.
10. Goodsell, D.S. Automated Docking of Flexible Ligands: Applications of Autodock. Journal of Molecular Recognition. 1996, 9(1): 1–5.
11. Jones, G., Willett, P., Glen, R.C., Leach, A.R. and Taylor, R. Development and validation of a genetic algorithm for flexible docking. J. Mol. Biol., 1997, 267(3):727–748.
12. PyMOL ™ (32 bit) – 1.3.0.0, Schrodinger LLC, 2010
13. Ramachandran, G.N., Ramakrishnan, C. and Sasisekharan, V. Conformation of polypeptides and proteins. J. Mol. Biol., 1963, 7: 95–99.
14. BIOVIA Discovery Studio 2016 Client, Version 16.1.0.
15. Gust, R., Gelbcke, M., Angermaier, B., Bachmann, H., Krauser, R. and Schönenberger, H. The stereoselectivity of antitumor active [1,2-diamino-1-phenylpropane]dichloroplatinum (II) complexes. Inorg. Chim. Acta, 1997, 264: 145–160.

*****